Intermetallics 18 (2010) 1772–1778

Contents lists available at ScienceDirect

Intermetallics

journal homepage: www.elsevier.com/locate/intermet

Martensitic features in Si doped $CeFe_2$ revealed by magnetization and transport study

Arabinda Haldar [a], K.G. Suresh [a,*], A.K. Nigam [b]

[a] Magnetic Materials Laboratory, Department of Physics, Indian Institute of Technology Bombay, Mumbai 400076, India
[b] Tata Institute of Fundamental Research, Homi Bhabha Road, Mumbai 400005, India

ARTICLE INFO

Article history:
Received 3 March 2010
Received in revised form
31 May 2010
Accepted 4 June 2010
Available online 29 June 2010

Keywords:
A. Magnetic intermetallics
A. Rare-earth intermetallics
B. Magnetic properties
B. Phase transformation
D. Martensitic structure

ABSTRACT

We report the effect of Si doping on the magnetization and transport behavior in $CeFe_2$. It is found that Si doping is able to stabilize the low temperature antiferromagnetic state in $CeFe_2$, resulting in a first order ferromagnetic to antiferromagnetic transition. The strong magnetostructural coupling in this system is found to give rise to martensitic features, which manifest in the magnetization and transport data. We show clear evidence of this influence through the multi-step magnetization behavior, unusual relaxation effect, thermal and magnetic history dependencies. The non-equilibrium magnetic state at low temperatures is also revealed by the fact that the magnetization steps can be induced with the help of an appropriate measurement protocol. Detailed magnetization relaxation studies have been carried out to understand the dynamics of magnetic phase transition. Martensitic scenario is also found to cause multi-step behavior in the magnetoresistance isotherms. By compiling all the distinct features in this system with those of other related systems, we conclude that this can be a model system that may contribute to understand the rich physics of phase separation and the martensitic scenario, both theoretically and experimentally.

1. Introduction

Interplay of more than one type of magnetic order and 'disorder-influenced' first order phase transition in a material give rise to a rich variety of magnetic and related properties. Many experimental and theoretical investigations have helped in framing various models to account for the observed behavior [1–4]. The first order transition followed by structural deformation/change in a magnetic material leads to different physical phenomena like supercooling/superheating, magnetization steps, phase coexistence, kinetic arrest, sluggish relaxation etc. Unusual step behavior across the metamagnetic transition seen in a few intermetallic compounds and a number of oxide materials have drawn a lot of interest recently [5–19]. Experimental studies in different classes of materials have been made to find out the reasons for the universality of these phenomena [20]. Various explanations based on random quenched disorder [17,21,22], martensitic character of phase transition [7,12,14,15], glassy behavior [23–25], first order phase transition [17,26–28] have been put forward.

Among the systems which show the above-mentioned magnetization behavior, doped $CeFe_2$ constitutes one of the most important classes of materials. $CeFe_2$ is unique among the RFe_2 (R = rare earth) series of compounds. Its saturation magnetization ($M_s = 2.4\mu_B$/f.u.) and Curie temperature ($T_C = 230$ K) are smaller compared to the compounds such as $LuFe_2$ ($T_C = 610$ K, $M_s = 2.9\mu_B$/f.u.) with its full 4*f* shell and YFe_2 ($T_C = 545$ K) which has no 4*f* electrons [29,30]. $CeFe_2$ is also known to possess a dynamic antiferromagnetic ground state, which gets stabilized with certain substituents such as Ru, Re, Al, Co, Ir, Os and Ga for Fe [6,15,31–34]. This series is known to undergo a structural change across the antiferromagnetic (AFM)-ferromagnetic (FM) transition [27,35–37]. Taking into account the similarities between Ga doped $CeFe_2$ and the well known phase-separated martensitic oxides, we have recently suggested that the martensitic scenario is present in the former case as well. Very sharp jumps in the magnetization isotherms at low temperatures have been observed in Ru, Re [17] and Ga [15] doped compounds. Unusual magnetization behavior in doped $CeFe_2$ compounds [15,17,27,38] has proved that this system can be a promising material to study the underlying physics of phase-separated systems where more than one phase (magnetic as well as structural) coexist and couple strongly with each other.

As part of our investigations on doped $CeFe_2$, recently, we could stabilize the AFM phase with Si substitution as well [39]. In a very recent paper, using in field and temperature variation of x-ray

* Corresponding author. Tel.: +91 22 25767559; fax: +91 22 25723480.
E-mail address: suresh@phy.iitb.ac.in (K.G. Suresh).

0966-9795/$ – see front matter © 2010 Elsevier Ltd. All rights reserved.
doi:10.1016/j.intermet.2010.06.001

diffraction, we have shown the structural change as a function of temperature as well as applied field in Ce(Fe,Si)$_2$ [40]. The crystal structure changes from cubic to rhombohedral as the magnetic state changes from FM to AFM. We could also see the coexistence of different structural and magnetic phases. With this clear evidence, we have focused our investigations to unravel the effect of the strong magnetostructural coupling on the magnetic and magneto-transport properties of Ce(Fe,Si)$_2$. This has been done by studying the dependence of these properties under different measurement protocols. By comparing our results with those of the well known phase-separated systems, we conclude that the present system also possesses phase coexistence and metastability associated with the first order phase transition. Dynamics associated with the first order transition is discussed in detail. Finally, we also give a comparative analysis on the effects of Ga and Si doping, with regard to the magnetization anomalies.

2. Experimental details

Polycrystalline compounds of Ce(Fe$_{1-x}$Si$_x$)$_2$ with $x = 0.01$, 0.025 and 0.05 were prepared by arc melting of the constituent elements: Ce (99.9%), Fe and Si (99.999%). All these elements were supplied by *Alfa Aesar*. The resulting ingots were turned upside down and remelted several times to ensure homogeneity. Weight losses were found to be less than 0.5%. The as-cast samples were annealed at 600 °C for 2 days, 700 °C for 5 days, 800 °C for 2 days and 850 °C for 1 day [31]. The structural analysis was performed by the Rietveld refinement of room temperature x-ray diffraction patterns (XRD). Magnetization (M) and resistivity (ρ) measurements in the temperature (T) range of 1.8–330 K and in fields (H) up to 90 kOe were carried out in the Physical Property Measurement System (PPMS-9 T). A few measurements were performed in the Squid magnetometer (MPMS-5 T and MPMS-7 T). Measurements have been taken in zero field cooled (ZFC), field cooled cooling (FCC) and field cooled warming (FCW) modes. In ZFC and FCW modes, the data were collected during warming while in FCC mode, it was collected during cooling. In the case of FCC and FCW modes, the cooling and the measuring fields were kept the same, unless otherwise mentioned.

3. Results

The Rietveld refinement of XRD has shown that Ce(Fe$_{1-x}$Si$_x$)$_2$ compounds, like the parent compound, possess the MgCu$_2$ type cubic structure with the space group $Fd\bar{3}m$. The lattice parameters (a) obtained from the refinement are 7.3020(3) Å for $x = 0.01$, 7.3033(4) Å for $x = 0.025$ and 7.3054(3) Å for $x = 0.05$. Table 1 gives the different structural parameters as obtained from the refinement for Ce(Fe$_{0.95}$Si$_{0.05}$)$_2$ compound.

Fig. 1(a) shows the variation of magnetization with temperature of all the compounds in a field of 500 Oe. M *vs.* T plot for CeFe$_2$ [15] has been shown for comparison. With substitution of Si, the fluctuating AFM state present in the parent compound gets stabilized for $x \geq 0.025$. The order–order (FM-AFM) transition occurs at 41 K for $x = 0.025$ and at 65 K for $x = 0.05$. As can be observed from the

Table 1
Structural parameters of Ce(Fe$_{0.95}$Si$_{0.05}$)$_2$ as obtained from the Rietveld refinement. At room temperature the structure is cubic (space group:$Fd\bar{3}m$). The unit cell dimension is: $a = 7.3054(3)$ Å.

Atom	Site	x	y	z	Occupancy
Ce	8a	0	0	0	0.042
Fe	16d	0.625	0.625	0.625	0.081
Si	16d	0.625	0.625	0.625	0.004

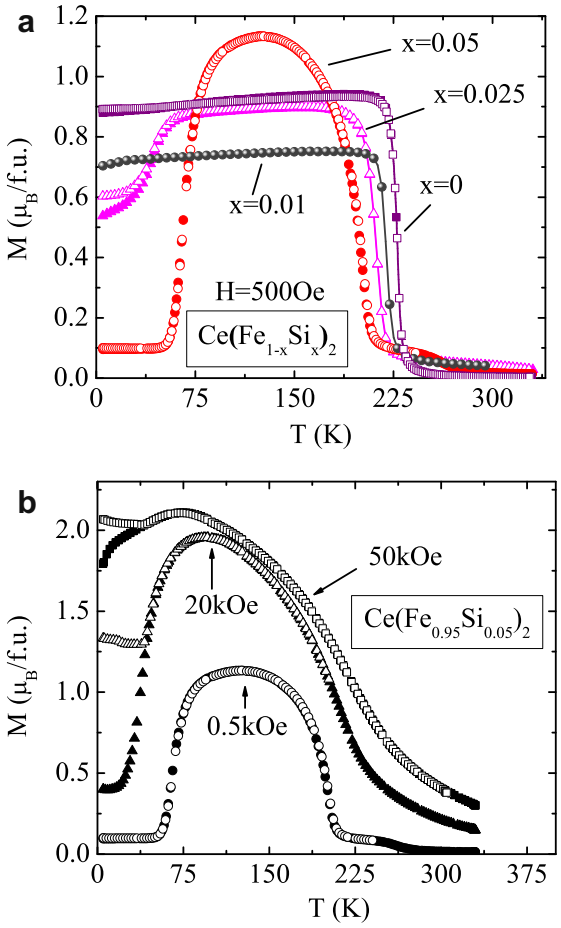

Fig. 1. (a) Temperature variation of ZFC (filled symbols) and FCW (open symbols) magnetization of Ce(Fe$_{1-x}$Si$_x$)$_2$ compounds. (b) Temperature dependence of ZFC and FCW magnetization of Ce(Fe$_{0.95}$Si$_{0.05}$)$_2$ in different applied magnetic fields.

Fig. 1(a), AFM ground state is partially stabilized in $x = 0.025$ whereas it is better stabilized in $x = 0.05$. Between the ZFC and FCW data, $x = 0.025$ shows some difference at low temperatures at $H = 0.5$ kOe but the compound with $x = 0.05$ does not show any such difference. This is another indication that the strength of AFM is stronger in $x = 0.05$. However, it is noteworthy that at higher fields, the ZFC and FCW data for $x = 0.05$ starts deviating from each other, as shown in Fig. 1(b). This behavior is also illustrated with the resistivity data shown later. In this respect, this system shows similarities with the recently reported Ce(Fe$_{0.96}$Ru$_{0.04}$)$_2$ system [23]. Due to the first order nature of the magnetic transition, there is supercooling of the FM phase to lower temperatures, in the case of field cooling. This is responsible for the increase in the FCC and FCW magnetization with field. Under ZFC, the supercooling is confined to a very narrow regime of temperature below the transition temperature and hence results in the bifurcation between the FCW and ZFC data [40].

To understand the type of glassiness in this compound we have carried out $M(T)$ measurement after cooling and heating in unequal fields [23]. For this, the measuring field ($H_{measure}$) was kept as 20 kOe, while the sample was cooled (H_{cool}) in 0, 10, 15, 20, 25, 30 kOe (Fig. 2). The dotted line shows the transition temperature which was estimated from dM/dT *vs.* T plot. The inset shows the $M(T)$ data at $H = 20$ kOe in different modes. Arrows in the Fig. 2 indicate the direction of the temperature change. It is to be noted here that the behavior of the plot is quite different when $H_{measure} > H_{cool}$ and $H_{measure} < H_{cool}$. In the former case, the magnetization is almost

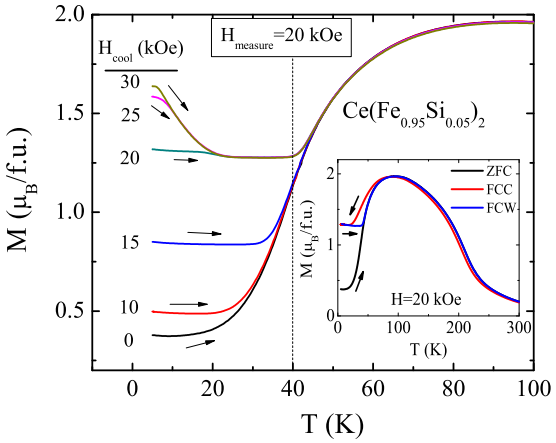

Fig. 2. Temperature dependence of magnetization in FCW mode at $H = 20$ kOe after cooling the sample in 0, 10, 15, 20, 25, 30 kOe magnetic field. Inset shows the $M(T)$ plot at $H = 20$ kOe in ZFC, FCC and FCW mode. Arrows indicate the direction of temperature change during measurement.

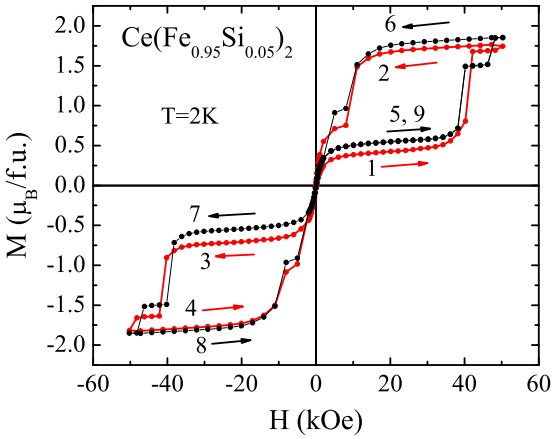

Fig. 3. Isothermal magnetization for $Ce(Fe_{0.95}Si_{0.05})_2$ at $T = 2$ K. Arrows show the field directions in which measurements have been carried out.

a constant upto the transition region, while in the latter case, the magnetization initially decreases as the temperature is increased, then shows a flat behavior before increasing again at the transition region. As mentioned earlier, in higher cooling fields (>20 kOe), more FM phase persists down to low temperatures in the non-equilibrium state, which decreases when $H_{measure}$ ($<H_{cool}$) is applied. This is in contrast to the observations in reentrant spin glass systems like $Au_{82}Fe_{18}$ and indicates magnetic glass type behavior [23].

Furthermore, comparing the behavior observed in Ga doped $CeFe_2$ [15], we find that 2.5% ($x = 0.025$) of Ga stabilizes the AFM phase well whereas a higher (5%) of Si is needed to obtain a fully AFM ground state. This indicates the fact that the nature of the substituting element plays an important role in the magnetic properties in this series. We believe that with various substituting elements, the structural and magnetic phase diagrams are different [31] and this factor accounts for the variations seen with different substitutions. In the subsequent sections, we highlight our results mainly on the compound with $x = 0.05$, as it presents the best scenario with regard to the AFM stabilization and the related effects.

Magnetization isotherms have been taken on all the compounds at very low temperatures, up to a maximum field of 90 kOe. It was found that the M (H) behavior of $x = 0.025$ and 0.05 compounds show metamagnetic transitions from AFM to FM phase, which was expected in view of the M vs. T data. Fig. 3 shows the M vs. H plots for $Ce(Fe_{0.95}Si_{0.05})_2$ for various field cycles at 2 K. The sample was zero field cooled from 325 K. Measurement was performed in a Squid magnetometer with a field step size of 2 kOe in the high field region. Application of field favors the final state to be ferromagnetic and depending on the strength of AFM, the metamagnetic transition occurs with increase in field. The magnetization increases only nominally in the low field region, but shows a sharp jump at about 38 kOe. It is important to note that the value of the critical field (H_c) depends on the details of the measurement procedure and the thermal and magnetic history of the sample, as will be shown later. Another feature that can be noticed from Fig. 3 is the fact that the virgin curve (first path) is outside the envelope curve (fifth path), similar to that in Ru, Re or Ga doped $CeFe_2$ [15,17]. But the notable difference in the present case compared to Ru/Re/Ga doping is that the magnetization steps are seen not only in the first loop, but in subsequent loops as well. This implies that the forced ferromagnetic state looses its stability as the field is reduced. It is also clear from Fig. 3 that the 8th and 9th loops coincide with 4th and 5th loops respectively, which is not the case with Ga doped compounds. These observations seem to suggest that the effect of kinetic arrest is less in the Si compounds. The reason for this may be the enhanced AFM strength in the Si doped compounds, mentioned above. This indication is confirmed by transport data (shown later) as well.

M (H) isotherms have been taken in different temperatures across both the transition regions and the Arrott's (M^2 vs. H/M) plots are shown in Fig. 4. The S-shaped behavior (Fig. 4(a)) of these plots also indicates the first order nature of the AFM-FM transition. It is also clear that the FM-paramagnetic (PM) transition is second order in nature (Fig. 4(b)). The variation of the magnetic entropy change calculated using the Maxwell's relation, [41] for the AFM-FM and FM-PM transition regimes is shown in Fig. 4(c). As expected, the entropy change is positive at the low temperature transition whereas it is negative in the FM-PM transition.

In order to further probe the dynamics of the magnetization growth in the AFM dominated regime, we have also studied the

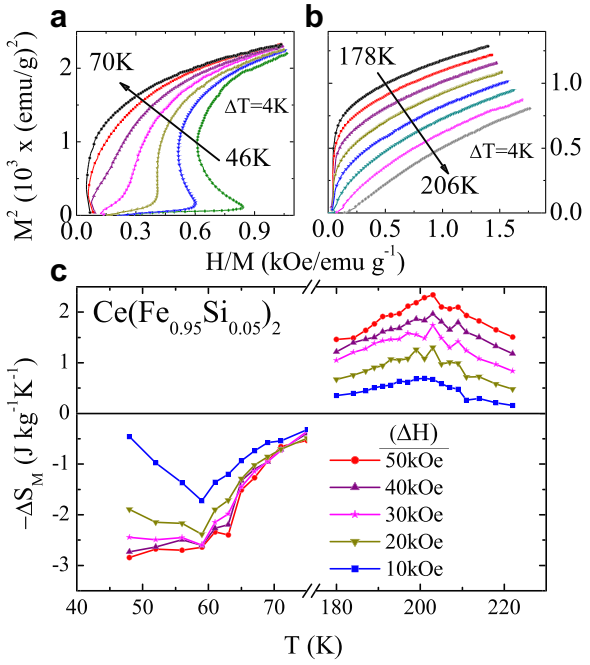

Fig. 4. Arrott's plots (a, b) and variation of magnetic entropy change with temperature (c) for $Ce(Fe_{0.05}Si_{0.05})_2$ compound.

variation of magnetization under different measurement protocols (using PPMS). Fig. 5 shows M (H) data taken in three different protocols; (a) with a sweep rate of 100 Oe/s at $T = 2$ K, (b) with a sweep rate of 10 Oe/s at $T = 1.9$ K and (c) in the interrupted sweep at $T = 1.9$ K where the scan was delayed for 2 h at six selected fields. A sharp step is observed in case (a) when the sweep rate is large, but it becomes smooth at slower sweep rate (case (b)). The temperature difference of 0.1 K between (a) and (b) is not expected to play any significant variation and essentially, the change seen between these two figures is purely attributable to the sweep rate difference. The absence of sharp steps in slow sweep rate can be explained from the martensitic picture [11,14,15]. The fact that the FM phase is cubic while the AFM phase is rhombohedral leads to the creation of martensitic strains as the system changes between the AFM and FM states [40]. Due to this, a slow change in the driving forces (field in this case) assists the system to transform slowly and progressively from a distorted phase to a more ordered phase. During this process the system finds enough time to overcome the elastic energy gradually across the two phases, which block the transition up to a certain critical field. It is noteworthy that these features can be observed even in squid measurement by adopting appropriate field steps. The influence of the driving force on the magnetization growth is a characteristic feature of martensitic behavior [11,14,15]. Fig. 5(c) shows the data in the interrupted sweep mode in which the fields (near the metamagnetic transition region) namely 37, 38, 39, 40, 41 and 42 kOe, were held constant for 2 h. Interestingly sharp steps are found at each of these fields, indicating that there exists an induction period for these steps to appear. From this plot, it is clear that steps can be induced by waiting for sufficient time durations, even when the field and the temperature are fixed. A similar observation has been reported in a few phase-separated oxides in which the martensitic effects are known to influence the magnetization behavior [11,19,24].

The growth of FM phase during the holding time (at constant field and temperature), in the interrupted sweep mode, is demonstrated in Fig. 6. This shows a rather sluggish relaxation and this type of behavior can be compared with the one observed in the case of manganites, shown by different authors [11,19,24]. Magnetic relaxation at different fixed fields can be well described by a stretched exponential of the type: $M_t(H) = M_0(H) + [M_\infty(H) - M_0(H)][1 - \exp\{-(t/\tau)^\alpha\}]$, where τ is the characteristic relaxation time and α is called stretching parameter that can range between 0 and 1 [11]. The fitting yielded the stretching parameter as about 0.5 and the characteristic relaxation time (τ) in the range of 1300–2700 s depending on the applied field. An anomaly in the normalized magnetization is observed for the holding field of 37 kOe (arrow in Fig. 6). The moments relax to different final values for different holding fields. As a consequence, the step sizes in M (H) depend on the holding fields and also on the wait time (here 2 h for each holding field). In general, the relaxation data indicates a glassy phase at low temperatures. This sluggish response of moment orientations in response to the external field, in other words the magnetic lag, is often defined as magnetic viscosity (S). The magnetic viscosity has been calculated using the relation: $S = (1/M_0) \times [\{dM/d(\log_{10} t)\}]$ [Ref. [42]]. The S across this region is shown in the inset of Fig. 6. It can be seen that S increases initially and at higher fields (above 41 kOe), it almost saturates. We conclude here that the observed variation of S is consistent with the field dependence of magnetization and that it can be attributed to the change in the fraction of antiferro (rhombohedral) and ferromagnetic (cubic) phases. This is also in agreement with the in-field x-ray diffraction data [40]. It may be noted that in the relaxation measurement we have only concentrated around the metastable region and we have obtained the value of S of the same order as reported by Deac et al. in $La_{0.250}Pr_{0.375}Ca_{0.375}MnO_3$ [42] and Rana et al. in $(La_{0.325}Tb_{0.125})(Ca_{0.3}Sr_{0.25})MnO_3$ [8].

As the transport behavior is quite sensitive to the magnetic state of the material, in order to find out the effect of the martensitic

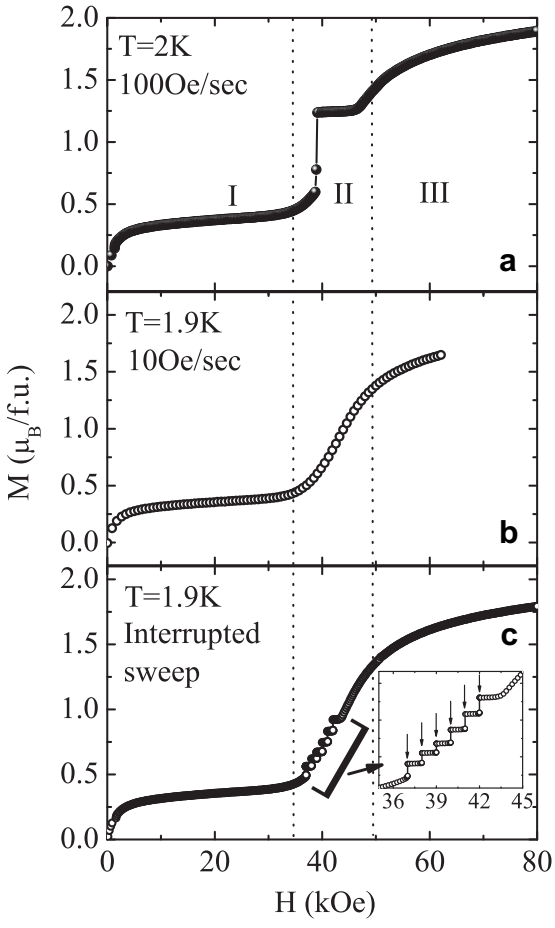

Fig. 5. Isothermal magnetization curves of $Ce(Fe_{0.95}Si_{0.05})_2$ showing the effect of the measurement protocol. Field sweep rates are (a) 100 Oe/s, (b) 10 Oe/s and (c) interrupted sweep where 37, 38, 39, 40, 41 and 42 kOe were held for 2 h each, with a field sweep rate of 100 Oe/s. Inset of (c) shows the enlarged part of selected region. Arrows indicate the positions where the field was kept constant for 2 h.

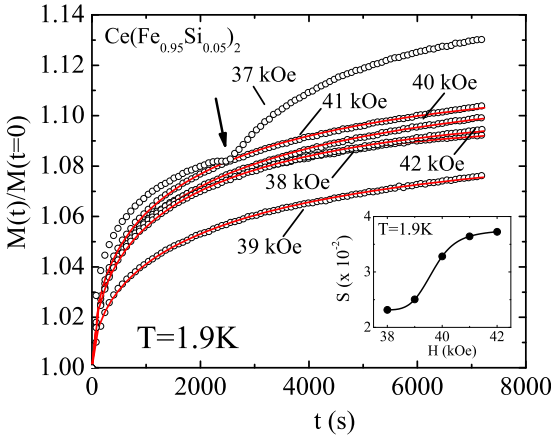

Fig. 6. Variations of normalized magnetization in $Ce(Fe_{0.95}Si_{0.05})_2$ with time at different holding fields. Arrow shows the jump in normalized magnetization for the holding field of 37 kOe. Inset shows the field dependence of magnetic viscosity (S) for $Ce(Fe_{0.95}Si_{0.05})_2$ at 1.9 K.

scenario on the transport properties, we have also studied the electrical resistivity variation in the present series. The electrical resistivity and magnetoresistance have been measured for the compounds with $x = 0.025$ and $x = 0.05$. Samples were subjected to thermal cycling from well above the FM-PM transition between successive measurements. In the resistivity data in zero field, there is a clear indication of a change in the slope at the PM-FM and FM-AFM transitions, as is evident from Fig. 7(a). The fact that the AFM ground state is better stabilized in $x = 0.05$ sample is supported by the resistivity data also. Resistivity data in 30 kOe in both the compounds clearly show that the system gradually converts to the field-induced FM phase. Field cooling in 30 kOe is able to suppress the AFM component completely even in $x = 0.05$, as revealed by the ρ-T plot.

It is very interesting to see the correlation between the magnetization and the resistivity data taken under different measurement protocols (ZFC, FCC and FCW), as is evident from Fig. 7(b). Distinct features of first order transition have been found in this data. A clear bifurcation in FCC and FCW data shows that FM-AFM transition during cooling and AFM-FM transition during heating occur at different temperatures which is an indication of supercooling (superheating) of FM (AFM) phase [26,27]. The structural distortion across the transition (as mentioned earlier) and the kinetics of transformation also contribute to the difference in the data collected with different measurement protocols. The bifurcation between ZFC and FCW increases with the increase in field, as observed in M *vs.* T plot. The resistivity at the lowest temperature is found to be less in the field cooled (FCC or FCW) modes as compared to that in the ZFC mode. This corroborates with the fact that more FM fraction, which has lower resistivity, is present in the former case. Therefore, it is quite clear that the temperature variation of magnetization and resistivity data under different protocols are in good agreement.

Magnetoresistance (MR) has been calculated using the relation$[(\rho(H) - \rho(0))/\rho(0)]$, in the ZFC mode [43]. It is to be noted here that, like the magnetization isotherms, MR isotherms also show multiple jumps during the field-induced AFM-FM transition in the case of $Ce(Fe_{0.95}Si_{0.05})_2$ (Fig. 8). Relief of strain across the AFM-FM transition causes the MR to change in a burst-like fashion as discussed under Fig. 5. For a better comparison, both these isotherms are plotted in Fig. 8. It is noteworthy that the critical fields where the sudden change occurs in both resistivity and magnetization are almost the same. At 2 K the critical field (where the abrupt change occurs) which transforms the low field AFM phase to the high field FM phase along path 1 is different compared to that in loop 2. This feature can also be attributed to the supercooling (superheating) of FM (AFM) phase below (above) critical field and indicates the metastable behavior which is the signature of first order transition. The fact that the envelope curve lies inside the virgin curve which indicates that some fraction of FM phase is arrested in the low field after cycling the field to zero. These types of features have been reported in Al doped $CeFe_2$, although no step

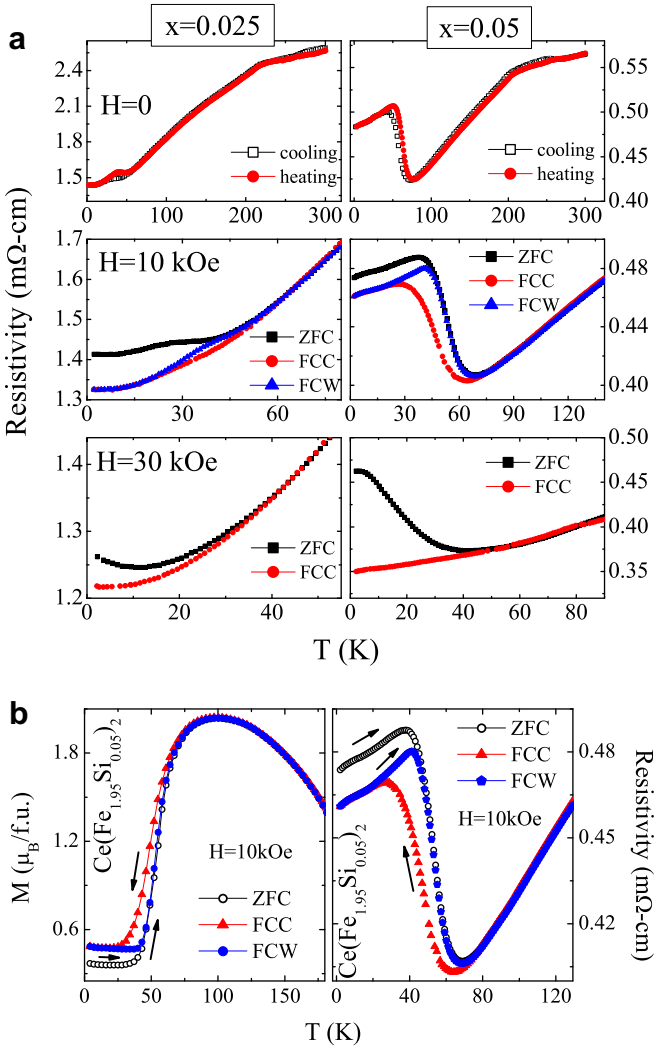

Fig. 7. (a) Temperature dependence of electrical resistivity at different fields in Ce$(Fe_{1-x}Si_x)_2$ compounds with $x = 0.025$ and $x = 0.05$. (b) Magnetization and resistivity data shown in ZFC, FCC and FCW modes at 10 kOe across the FM-AFM region in $x = 0.05$. Arrow shows the measurement direction.

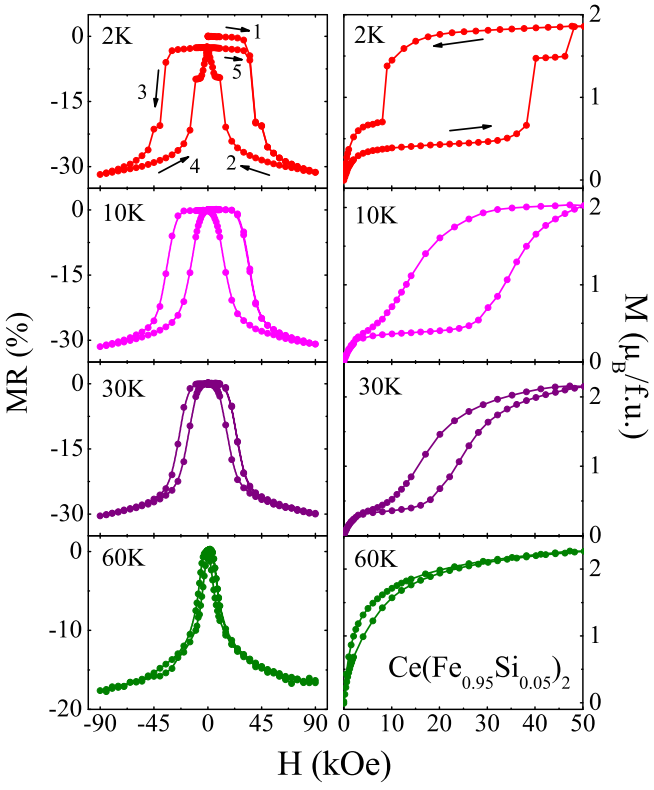

Fig. 8. Variation of magnetoresistance (left panel) and magnetization (right panel) with field at different temperatures for $Ce(Fe_{0.95}Si_{0.05})_2$. Arrows shows the direction of measurement.

behavior was found [26,27]. The absence of step behavior in Al doping may be due to large overlap between different phases, which gives rise to a broad transition. With increase in temperature, the hysteresis in the MR diminishes. The same trend was seen in the magnetization data as well. A large MR value of 33% is obtained across AFM-FM transition at low temperatures which is comparable with other doped $CeFe_2$ compounds [26,27,43,44]. However, there are no reports on the observation of steps in MR isotherms in doped $CeFe_2$, though such an observation is reported in the case of manganites [7]. Therefore, the step behavior seen in the present case is of importance as it clearly establishes the correlation between the magnetization anomalies and the transport properties.

The left panel in Fig. 9 shows that in the field cooled mode also, the steps in the MR isotherms appear at the same fields as in the ZFC case. Moreover, the step size is almost independent of the cooling field. More or less the same features can be seen in the magnetization isotherms as well (right panel, Fig. 9). These observations imply that the AFM coupling is very strong in the ground state so that when cooling field is reduced to zero (i.e., at the start of the measurement) at the measurement temperature, the system reverts to the predominantly AFM state. Therefore, it is clear that the cooling field is able to assist the AFM-FM conversion only partially. This is in sharp contrast to the observation seen in Ga doped $CeFe_2$ in which the step size and the position in the magnetization isotherms were found to change with cooling field. This again highlights the role of dopants in determining the properties in $CeFe_2$ series. In this context, it is to be mentioned that in martensitic systems based on full Heusler alloys, the supercooled high temperature phase achieved by field cooling gets arrested strongly to such an extent that even when the cooling field is reduced to zero, the supercooled phase does not relax without heating [45].

4. Discussion

The results presented in the above section show that both the magnetization and the electrical resistivity behavior in Si doped $CeFe_2$ seem to be influenced by the martensitic strains associated with the AFM-FM transition. As mentioned earlier, the structural change associated with this transition [40] and the first order nature of it leads to a phase-separated scenario. It is important to note that when clusters form in the matrix phase, an elastic-misfit strain energy is generated because of volume or/and shape incompatibilities between the FM (cluster) and the AFM (matrix) phase (see inset of Fig. 2 of Ref. [40]). In the martensitic picture, the formation of FM phase by this discontinuous phase transformation requires the nucleation of the new (FM) phase in highly localized regions in which the heterogeneous nucleation takes place [46]. The quenched disorder due to small doping (here silicon) concentration inside the matrix and also the defects like grain boundaries, grain edges and grain corners in a polycrystalline compound can act as special sites. This process generally occurs in three stages. Stage I is the incubation period (as seen in Fig. 5(c)) in which the AFM phase is metastable. New clusters of very small sizes, which are precursors to the final stable FM phase continuously form and decompose in the matrix. Stage II, can be denoted as metamagnetic region where the distribution of these small clusters evolves with field and/or time to produce larger clusters. Extremely sharp steps have been observed across this transition before the final stable state is reached. The reason for the step behavior may be as follows. Elastic-misfit strain energy as discussed above acts as a barrier to the nucleation [46]. Externally applied magnetic field favors FM fraction (cubic) within the matrix (rhombohedral) and system releases its strain energy across the transition. It is justified to assume here that depending on the experimental conditions this release of strain energy may occur in a burst-like fashion. As a consequence, the moments suddenly jump to a certain magnetization value producing ultra sharp steps across this order–order transition as clearly seen in Fig. 5(a). In stage III, the rate of nucleation is retarded and formation of new stable phase is almost complete. Final stable FM phase is less likely to revert back to the matrix AFM phase. It is observed that when we decrease the magnetic field, the magnetization does not follow the same path. This may be understood by assuming that some of the largest of these clusters evolve into stable nuclei of FM phase and get arrested in the system [17,26]. It is theoretically proposed that the interplay of more than one order parameter in a system can lead to a rich variety of their properties [2]. The competition between the AFM and the FM states associated with the rhombohedral and the cubic structures causes anomalies in the physical properties in the present system. The general features observed in the field-induced first order magnetostructural phase transition here appear to be the universal features of martensitic transformations seen in a variety of systems.

Detailed relaxation measurement and the M–T data indicate glassy behavior at low temperatures. Presence of characteristic relaxation time has been shown from the stretched exponential behavior, as seen in manganites [11,19,24]. Using VSM and squid data, we find that the measurement protocol plays a crucial role in determining the properties of this phase-separated system [11,14]. This measurement protocol dependence also indicates martensitic type behavior in this system. Comparing the results obtained in the Ga and Si doping in $CeFe_2$, it can be mentioned that the substituting element plays an important role in the stabilization of the AFM phase and the anomalous behavior in the physical properties. Although the qualitative behavior in all the doped $CeFe_2$ compounds is similar, there are certain differences in magnetization and resistivity data among various dopants such as Ru, Al, Ga, Si. It opens up a challenge to elucidate the effect of the dopants by investigating their electronic structural and micro-structural variations.

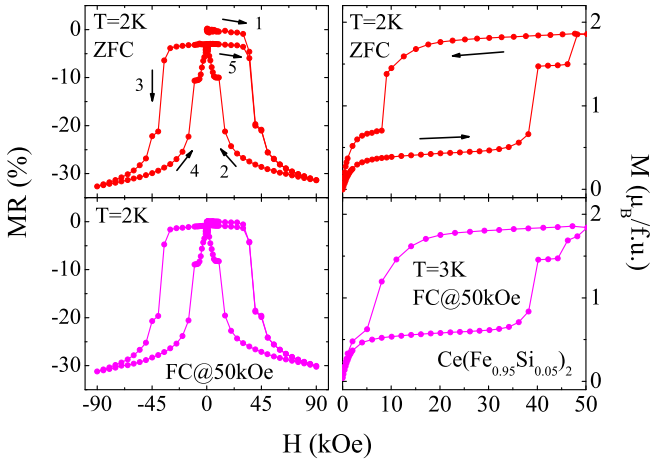

Fig. 9. The left panel shows magnetoresistance *vs.* field of $Ce(Fe_{0.95}Si_{0.05})_2$ taken in zero field cooled and field cooled (at 50 kOe) modes. The right panel shows the corresponding magnetization isotherms.

5. Conclusion

Detailed magnetization and resistivity measurements have been performed in Si doped $CeFe_2$ compounds. It is found that Si doping is able to stabilize the low temperature antiferromagnetism in $CeFe_2$. The results show the occurrence of multiple steps in the

magnetization and magnetoresistance isotherms. As in the case of phase-separated manganites, these steps are found to be dependent on the experimental protocols used, which indicates that this system displays martensitic behavior. Presence of incubation time and variation of magnetic viscosity have been discussed to understand the dynamics of the magnetization behavior. Magnetization data indicate that the magnetic state of the system is of glassy nature at low temperatures. The results obtained in this system clearly present all the features characteristic of the phase-separated systems in which the interplay between more than one order parameter is the key to all the anomalous properties. Reproducibility of the steps and strong dependence of the properties on extrinsic parameters open up a lot of opportunity to study the kinetics of these materials in further detail. All the findings in the present study are found to be in conformity with the detailed field and temperature variation of XRD studies reported in this system, highlighting the underlying martensitic features.

Acknowledgement

KGS and AKN thank Board of Research in Nuclear Sciences (Department of Atomic Energy, Govt. of India) for providing the financial support for carrying out this work. The authors also thank Mr. Devendra D. Buddhikot for his help in the resistivity measurements.

References

[1] Imry Y, Ma SK. Phys Rev Lett 1975;35:1399.
[2] Imry Y. J Phys C Solid State Phys 1975;8:567.
[3] Westphal V, Kleemann W, Glinchuk MD. Phys Rev Lett 1992;68:847.
[4] Stryjewski E, Giordano N. Adv Phys 1977;26:487.
[5] Hebert S, Hardy V, Maignan A, Mahendiran R, Hervieu M, Martin C, et al. J Solid State Chem 2002;165:6;
Solid State Commun 2002;122:335.
[6] Maignan A, Hébert S, Hardy V, Martin C, Hervieu M, Raveau B. J Phys Condens Matter 2002;14:11809.
[7] Mahendiran R, Maignan A, Hebert S, Martin C, Hervieu M, Raveau B, et al. Phys Rev Lett 2002;89:286602.
[8] Rana DS, Kuberkar DG, Malik SK. Phys Rev B 2006;73:064407.
[9] Rana DS, Malik SK. Phys Rev B 2006;74:052407.
[10] Nair S, Nigam AK, Narlikar AV, Prabhakaran D, Boothroyd A. Phys Rev B 2006;74:132407.
[11] Liao D, Sun Y, Yang R, Li Q, Cheng Z. Phys Rev B 2006;74:174434.
[12] Hardy V, Majumdar S, Lees MR, Paul DMcK, Yaicle C, Hervieu M. Phys Rev B 2004;70:104423.
[13] Woodward FM, Lynn JW, Stone MB, Mahendiran R, Schiffer P, Mitchell JF, et al. Phys Rev B 2004;70:174433.
[14] Hardy V, Majumdar S, Crowe SJ, Lees MR, Paul DMcK, Herve L, et al. Phys Rev B 2004;69:020407(R).
[15] Haldar A, Suresh KG, Nigam AK. Phys Rev B 2008;78:144429.
[16] Levin EM, Gschneidner Jr KA, Pecharsky VK. Phys Rev B 2002;65:214427.
[17] Roy SB, Chattopadhyay MK, Chaddah P. Phys Rev B 2005;71:174413.
[18] Ouyang ZW, Pecharsky VK, Gschneidner Jr KA, Schlagel DL, L0ograsso TA. Phys Rev B 2007;76:134406.
[19] Hardy V, Maignan A, Hebert S, Yaicle C, Martin C, Hervieu M, et al. Phys Rev B 2003;68:220402(R).
[20] Roy SB, Chaddah P, Pecharsky Jr VK, Gschneidner KA. Acta Materialia 2008;56:5895.
[21] Kimura T, Tomioka Y, Kumai R, Okimoto Y, Tokura Y. Phys Rev Lett 1999;83:3940.
[22] Fisher LM, Kalinov AV, Voloshin IF, Babushkina NA, Khomskii DI, Zhang Y, et al. Phys Rev B 2004;70:212411.
[23] Roy SB, Chattopadhyay MK. Phys Rev B 2009;79:052407.
[24] Wu T, Mitchell JF. Phys Rev B 2004;69:100405(R).
[25] Chaddah P, Kumar Kranti, Banerjee A. Phys Rev B 2008;77:100402(R).
[26] Singh KJ, Chaudhary S, Chattopadhyay MK, Manekar MA, Roy SB, Chaddah P. Phys Rev B 2002;65:094419.
[27] Manekar MA, Chaudhary S, Chattopadhyay MK, Singh KJ, Roy SB, Chaddah P. Phys Rev B 2001;64:104416.
[28] Chattopadhyay MK, Manekar MA, Pecharsky AO, Pecharsky VK, Gschneidner Jr KA, Moore J, et al. Phys Rev B 2004;70:214421.
[29] Eriksson O, Nordstrom Lars, Brooks MSS, Johansson Borje. Phys Rev Lett 1988;60:2523.
[30] Giorgetti C, Pizzini S, Dartyge E, Fontaine A, Baudelet F, Brouder C, et al. Phys Rev B 1993;48:12732.
[31] Roy SB, Coles BR. J Phys Condens Matter 1989;1:419.
[32] Roy SB, Coles BR. Phys Rev B 1989;39:9360.
[33] Rajarajan AK, Roy SB, Chaddah P. Phys Rev B 1997;56:7808.
[34] Haldar A, Suresh KG, Nigam AK, Coelho AA, Gama S. J Phys Condens Matter 2009;21:496003.
[35] Chattopadhyay MK, Roy SB, Nigam AK, Sokhey KJS, Chaddah P. Phys Rev B 2003;68:174404.
[36] Kennedy SJ, Coles BR. J Phys Condens Matter 1990;2:1213.
[37] Sokhey JS, Chattopadhyay MK, Nigam AK, Roy SB, Chaddah P. Solid State Commun 2004;129:19.
[38] Haldar A, Singh Niraj K, Mudryk Ya, Suresh KG, Nigam AK, Pecharsky VK. J Appl Phys 2010;107:09E133.
[39] Haldar A, Suresh KG, Nigam AK. J Phys Conf Ser 2010;200:032021.
[40] Haldar A, Singh NK, Mudryk Ya, Suresh KG, Nigam AK, Pecharsky VK. Solid State Commun 2010;150:879–83.
[41] Provenzano V, Shapiro AJ, Shull RD. Nature (London) 2004;429:853.
[42] Deac IG, Diaz SV, Kim BG, Cheong S-W, Schiffer P. Phys Rev B 2002;65:174426.
[43] Fukuda H, Fujii H, Kamura H, Hasegawa Y, Ekino T, Kikugawa N, et al. Phys Rev B 2001;63:054405.
[44] Kunkel HP, Zhou XZ, Stampe PA, Cowen JA, Williams Gwyn. Phys Rev B 1996;53:15099.
[45] Ito W, Ito K, Umetsu RY, Kainuma R, Koyama K, Watanabe K, et al. Appl Phys Lett 2008;92:021908.
[46] Balluffi RW, Allen SM, Carter WC. Kinetics of materials. Hoboken: Wiley; 2005.